



**University of  
Zurich**<sup>UZH</sup>

**Zurich Open Repository and  
Archive**

University of Zurich  
University Library  
Strickhofstrasse 39  
CH-8057 Zurich  
[www.zora.uzh.ch](http://www.zora.uzh.ch)

---

Year: 2017

---

## **Targeting BET proteins improves the therapeutic efficacy of BCL-2 inhibition in T-cell acute lymphoblastic leukemia**

Peirs, S ; Frismantas, V ; Matthijssens, F ; Van Looche, W ; Pieters, T ; Vandamme, N ; Lintermans, B ; Dobay, M P ; Berx, G ; Poppe, B ; Goossens, S ; Bornhauser, B C ; Bourquin, J-P ; Van Vlierberghe, P

**Abstract:** Inhibition of anti-apoptotic BCL-2 has recently emerged as a promising new therapeutic strategy for the treatment of a variety of human cancers, including leukemia. Here, we used T-cell acute lymphoblastic leukemia as a model system to identify novel synergistic drug combinations with the BH3 mimetic venetoclax (ABT-199). In vitro drug screening in primary leukemia specimens that were derived from patients with high risk of relapse or relapse and cell lines revealed synergistic activity between venetoclax and the BET bromodomain inhibitor JQ1. Notably, this drug synergism was confirmed in vivo using T-ALL cell line and patient-derived xenograft models. Moreover, the therapeutic benefit of this drug combination might, at least in part, be mediated by an acute induction of the pro-apoptotic factor BCL2L11 and concomitant loss of BCL-2 upon BET bromodomain inhibition, ultimately resulting in an enhanced binding of BIM (encoded by BCL2L11) to BCL-2. Altogether, our work provides a rationale to develop a new type of targeted combination therapy for selected subgroups of high-risk leukemia patients. Leukemia accepted article preview online, 11 January 2017. doi:10.1038/leu.2017.10.

DOI: <https://doi.org/10.1038/leu.2017.10>

Posted at the Zurich Open Repository and Archive, University of Zurich

ZORA URL: <https://doi.org/10.5167/uzh-131567>

Journal Article

Accepted Version

Originally published at:

Peirs, S; Frismantas, V; Matthijssens, F; Van Looche, W; Pieters, T; Vandamme, N; Lintermans, B; Dobay, M P; Berx, G; Poppe, B; Goossens, S; Bornhauser, B C; Bourquin, J-P; Van Vlierberghe, P (2017). Targeting BET proteins improves the therapeutic efficacy of BCL-2 inhibition in T-cell acute lymphoblastic leukemia. *Leukemia*, 31(10):2037-2047.

DOI: <https://doi.org/10.1038/leu.2017.10>

**Targeting BET proteins improves the therapeutic efficacy of BCL-2 inhibition in T-cell acute lymphoblastic leukemia**

S Peirs, V Frismantas, F Matthijssens, W Van Looke, T Pieters, N Vandamme, B Lintermans, M P Dobay, G Berx, B Poppe, S Goossens, B C Bornhauser, J-P Bourquin, P Van Vlierberghe

**Cite this article as:** S Peirs, V Frismantas, F Matthijssens, W Van Looke, T Pieters, N Vandamme, B Lintermans, M P Dobay, G Berx, B Poppe, S Goossens, B C Bornhauser, J-P Bourquin, P Van Vlierberghe, Targeting BET proteins improves the therapeutic efficacy of BCL-2 inhibition in T-cell acute lymphoblastic leukemia, *Leukemia* accepted article preview 11 January 2017; doi: [10.1038/leu.2017.10](https://doi.org/10.1038/leu.2017.10).

This is a PDF file of an unedited peer-reviewed manuscript that has been accepted for publication. NPG are providing this early version of the manuscript as a service to our customers. The manuscript will undergo copyediting, typesetting and a proof review before it is published in its final form. Please note that during the production process errors may be discovered which could affect the content, and all legal disclaimers apply.

Received 3 June 2016; revised 2 December 2016; accepted 12 December 2016;  
Accepted article preview online 11 January 2017

**Targeting BET proteins improves the therapeutic efficacy of BCL-2 inhibition in T-cell acute lymphoblastic leukemia**

Sofie Peirs<sup>1,2,\*</sup>, Viktoras Frismantas<sup>3,\*</sup>, Filip Matthijssens<sup>1,2</sup>, Wouter Van Loocke<sup>1,2</sup>, Tim Pieters<sup>1,2,4,5</sup>, Niels Vandamme<sup>2,4,5</sup>, Béatrice Lintermans<sup>1,2</sup>, Maria Pamela Dobay<sup>6</sup>, Geert Berx<sup>2,4,5</sup>, Bruce Poppe<sup>1,2</sup>, Steven Goossens<sup>1,2,4,5</sup>, Beat C Bornhauser<sup>3</sup>, Jean-Pierre Bourquin<sup>3,\*\*</sup> and Pieter Van Vlierberghe<sup>1,2,\*\*</sup>

<sup>1</sup>Center for Medical Genetics, Ghent University, Ghent, Belgium

<sup>2</sup>Cancer Research Institute Ghent (CRIG), Ghent, Belgium

<sup>3</sup>Department of Pediatric Oncology, Children's Research Centre, University Children's Hospital Zurich, Zurich, Switzerland

<sup>4</sup>Molecular and Cellular Oncology Lab, VIB Inflammation Research Center, Ghent University, Ghent, Belgium

<sup>5</sup>Department of Biomedical Molecular Biology, Ghent University, Ghent, Belgium

<sup>6</sup>Swiss Institute of Bioinformatics (SIB), Lausanne, Switzerland

\* SP and VF contributed equally to this work

\*\* JPB and PVV contributed equally to this work

**Running title**                      Combination of venetoclax and JQ1 in T-ALL

**Correspondence**

Jean-Pierre Bourquin, PhD

University Children's Hospital Zurich

Department of Pediatric Oncology

Children's Research Centre

August-Forelstrasse 1

8032 Zurich, Switzerland

Tel: +41 44 266 7304

Email: Jean-Pierre.Bourquin@kispi.uzh.ch

**Conflict of interest**

The authors declare no conflict of interest.

## Abstract

Inhibition of anti-apoptotic BCL-2 has recently emerged as a promising new therapeutic strategy for the treatment of a variety of human cancers, including leukemia. Here, we used T-cell acute lymphoblastic leukemia as a model system to identify novel synergistic drug combinations with the BH3 mimetic venetoclax (ABT-199). *In vitro* drug screening in primary leukemia specimens that were derived from patients with high risk of relapse or relapse and cell lines revealed synergistic activity between venetoclax and the BET bromodomain inhibitor JQ1. Notably, this drug synergism was confirmed *in vivo* using T-ALL cell line and patient-derived xenograft models. Moreover, the therapeutic benefit of this drug combination might, at least in part, be mediated by an acute induction of the pro-apoptotic factor *BCL2L11* and concomitant loss of BCL-2 upon BET bromodomain inhibition, ultimately resulting in an enhanced binding of BIM (encoded by *BCL2L11*) to BCL-2. Altogether, our work provides a rationale to develop a new type of targeted combination therapy for selected subgroups of high-risk leukemia patients.

## Introduction

T-cell acute lymphoblastic leukemia (T-ALL) arises from the malignant transformation of T-cell progenitors and accounts for about 15% of childhood and 25% of adult ALL cases(1). The cure rate for childhood T-ALL has steadily increased over the past decades, with current survival rates reaching approximately 85%(2, 3). Although these numbers are high, the clinical perspective for children that fail induction therapy or suffer from relapsed disease remains extremely poor, with only a 7-23% subset of relapsed T-ALL patients surviving beyond 3 to 5 years after the initial diagnosis(4). Compared to childhood leukemia, the clinical picture for adult T-ALL is even worse, with high relapse rates and long-term disease-free survival of about 40%(5-7). Altogether, these figures suggest that better and less toxic treatment strategies are urgently required to further improve the clinical management of childhood and adult T-ALL patients.

Recently, we and other research groups reported promising therapeutic activity for venetoclax (ABT-199), a highly specific inhibitor of the anti-apoptotic protein BCL-2, in immature subtypes of human T-ALL(8-10). Nevertheless, venetoclax sensitivity is variable between different T-ALL patient samples and the emergence of resistance to venetoclax(11-13) as well as the occurrence of dose-limiting toxicities(14) provides a rationale for the evaluation of venetoclax as part of a combination therapy. Indeed, previous studies have shown that venetoclax can synergize with conventional chemotherapeutic agents in human T-ALL, including doxorubicin, L-asparaginase, dexamethasone and cytarabine(8, 9). Venetoclax has recently also been approved by the FDA for the treatment of chronic lymphocytic leukemia (CLL). Indeed, clinical trials demonstrated progress-free survival in more than two thirds of relapsed CLL patients(14), including poor prognostic CLL patients that carry a 17p deletion(15). Nevertheless, complete remission remained uncommon(14), further reinforcing the need for the evaluation of combined therapeutic strategies.

Bromodomains of the bromodomain and extra-terminal (BET) protein family recognize  $\epsilon$ -N-acetylation of lysine residues on histone tails. BRD4 is an important BET protein that recruits the positive transcription elongation factor complex (P-TEFb) to acetylated chromatin(16). The transcriptional coactivators BRD4 and Mediator co-occupy enhancers and promoters of active genes and are enriched at large stretches of enhancer sequences, often termed super-enhancers(17-19). Notably, these enhancers regulate the expression of critical oncogenes in a variety of human cancers, providing a rationale for the use of BET bromodomain inhibitors, such as JQ1, as powerful anti-cancer agents(17-19). Also in T-ALL, BET bromodomain inhibitors have shown therapeutic efficacy in a number of *in vitro* and *in vivo* model systems and were shown to inhibit the expression of the T-ALL oncogene *MYC*(20-22). In addition, super-enhancers have been identified in a panel of T-ALL cell lines near putative oncogenes, including *MYB*, *TAL1*, *CDK6* and *NOTCH1*(18).

In this study, we identified synergistic drug combinations with the BH3 mimetic venetoclax in the context of human T-ALL. Most notably, we show that combined targeting of BCL-2 and BET bromodomain proteins synergistically affects leukemic tumor growth in T-ALLs that were resistant to conventional chemotherapeutic agents.

## Materials and methods

### Primary patient samples

Primary human ALL cells were recovered from cryopreserved bone marrow aspirates of patients enrolled in the ALL-BFM 2000, 2009 and ALL-REZ-BFM 2002 study. Informed consent was given in accordance with the Declaration of Helsinki and the ethics commission of the Kanton Zurich (approval number 2014-0383). Samples were classified as standard risk (SR), medium risk (MR), high risk (HR), very high risk (VHR) or relapse samples (R) according to the clinical criteria used in ALL-BFM 2000(23).

**Drug-screening platform**

The *in vitro* drug response of T-ALL primary patient samples was assessed in co-culture with hTERT-immortalized primary bone marrow mesenchymal stromal cells (MSC) as described previously (23). Details are provided in the supplementary data.

**Cell lines**

Cell lines were purchased from the DSMZ repository (Braunschweig, Germany), except for CUTLL1 (gift Prof. Adolfo Ferrando, Columbia University) and KOPTK1 (gift Prof. Hans-Guido Wendel, Memorial Sloan Kettering Cancer Center). Cells were cultured in RPMI 1640 medium (Life Technologies, Carlsbad, CA, USA; 52400-025) supplemented with 10% or 20% FBS, 100 U/ml penicillin, 100 µg/ml streptomycin (Life Technologies, 15140-148), 100 µg/ml kanamycin sulfate (Life Technologies, 15160-047) and 2 mM L-glutamine (Life Technologies, 25030024) at 37°C with 5% CO<sub>2</sub>.

***In vitro* evaluation of synergism between venetoclax and JQ1 in human T-ALL cell lines and primary samples**

The treatment of the cell lines with venetoclax (BioVision, Milpitas, CA; 2253-1) and/or (+)-JQ1 (BPS Bioscience, San Diego, CA, USA; 27401) and viability measurements via the CellTiter Glo Viability assay (Promega, Madison, WI, USA) have previously been described in Peirs et al.(8) CalcuSyn software (Biosoft, Cambridge, United Kingdom) was used to calculate the combination index (CI) with the Chou-Talalay method. The reported CI is the average of the values obtained at the ED<sub>50</sub>, ED<sub>75</sub> and ED<sub>90</sub> point. Primary patient samples co-titration experiments were performed for selected drugs. T-ALL cell plates were prepared and handled in the same manner as for drug combination screening described above. Selected drugs in combination with venetoclax were dispensed using Tecan D300 digital dispenser in a concentration matrix. The concentration range tested for venetoclax and JQ-1 were determined for each patient based on initial drug response screening. CI was calculated using Chou-Talalay method as implemented in R package (<https://github.com/xtmgah/DDCV>).



**Western blot**

Western blot analysis was performed as previously described(8). The primary antibodies used were Bcl-2 antibody (C-2) (1:500, Santa Cruz Biotechnology, Dallas, TX, USA; sc-7382), PARP-1 antibody (F-2) (1:1000, Santa Cruz Biotechnology, sc-8007), BIM antibody (1:1000, EMD Millipore, Darmstadt, Germany; AB17003),  $\beta$ -actin antibody (1:10000, Sigma-Aldrich, Saint Louis, MO, USA; Clone AC-75, A2228) and  $\alpha$ -tubulin antibody (1:10000, Sigma-Aldrich, T5168). The detection of the blots was done with ChemiDoc-It Imaging System (UVP, Upland, CA, USA). Densitometric analysis of the protein bands was performed using ImageJ (NIH, Bethesda, MD, USA). Images have been cropped for presentation.

**AnnexinV/PI staining**

FITC Annexin V Apoptosis Detection Kit I (BD Biosciences, San Jose, CA, USA; 556547) was used and samples were measured on the S3 cell sorter (Bio-Rad, Hercules, California, USA).

**Mice experiments**

Female nonobese diabetic/severe combined immunodeficient  $\gamma$  (NSG) mice were injected in the tail vein with 150 $\mu$ l PBS containing  $5 \times 10^6$  luciferase-positive LOUCY cells(8),  $5 \times 10^6$  ALL-SIL cells or  $1 \times 10^6$  cells from a secondary xenograft of patient T-VHR-26. Engraftment of the cells was followed by bioluminescence imaging as previously described(8) or by measuring the percentage of leukemic cells in the blood. Once there was clear engraftment (day 0), mice were randomly divided into four groups (control, venetoclax, JQ1 and combination) and treatment was started. Mice received daily 50mg venetoclax/kg body weight via oral gavage and/or 50mg JQ1/kg body weight via intraperitoneal injection. Venetoclax (Axon Medchem, Groningen, The Netherlands) was formulated in 60% phosal 50 propylene glycol, 30% polyethylene glycol 400 and 10% ethanol. (+)-JQ1 (MedChem Express, South Brunswick Township, NJ, USA) was formulated in 10% DMSO and 90% of a 10% 2-hydroxypropyl- $\beta$ -cyclodextrin solution. At the end of the treatment period, blood was taken and mice were sacrificed. The percentage of leukemic cells was analyzed by staining the cells with an PE-

labeled antibody for human CD45 (hCD45) (Miltenyi Biotec, Bergisch Gladbach, Germany; 130-098-141), performing red blood cell lysis and measuring the percentage on a LSRII flow cytometer using FACSDiva software (BD Bioscience). The ethical committees on animal welfare at Ghent University Hospital and University Children's Hospital Zurich approved all animal experiments.

### **Gene expression profiling and GSEA**

LOUCY cells were treated with DMSO or (+)-JQ1. Three biological replicates of this treatment were performed and RNA was isolated using the miRNeasy mini kit (Qiagen, Venlo, The Netherlands) with on-column DNase digestion. RNA quality was evaluated by the Experion RNA StdSens analysis kit (Bio-Rad). RNA was amplified and labeled using the Low Input Quick Amp Labeling Kit, One Color (Agilent Technologies, Santa Clara, CA, USA; 5190-2305) and hybridized with the Gene Expression Hybridization Kit (Agilent Technologies, 5188-5242) to the SurePrint G3 Human Gene Expression Microarray G4851A (design ID 028004, Agilent Technologies). Normalization of microarray intensities was done using the variance stabilization and calibration (VSN, version 3.30.0) package in R (version 3.0.2). Only probes with a signal 10% higher than the negative control probes were considered for analysis. Differential expression analysis was performed using the limma package (version 3.18.13) with p-value adjustment using the Benjamini and Hochberg method. The design matrix took into account the pairing information of the data. Enrichment analysis was performed with the MSigDB c2 gene sets collection using the GSEA desktop application (Broad Institute, version v2.2.0) run with the default parameters and with gene set permutations. The data have been deposited in NCBI's Gene Expression Omnibus(24) and are accessible through GEO Series accession number GSE81918.

### **Real-time quantitative PCR (RT-qPCR)**

The miRNeasy mini kit (Qiagen) and the RNase-Free Dnase set (Qiagen) were used to isolate RNA. For determination of mRNA levels, cDNA synthesis was performed with the iScript Advanced cDNA synthesis kit (Bio-Rad). The SsoAdvanced Universal SYBR Green Supermix (Bio-Rad) was used for the PCR reactions. Every sample was analyzed in duplicate and the gene expression was normalized

against 3 housekeeping genes. For quantification of mature miRNAs, the miScript II RT kit (Qiagen) and target-specific miScript Primer Assays (Qiagen) together with the miScript SYBR Green PCR Kit were used. All RT-qPCR reactions were run on the LightCycler 480 (Roche, Vilvoorde, Belgium) and qBasePLUS software (Biogazelle, Zwijnaarde, Belgium) was used for analysis. Primer sequences and miScript Primer Assays are listed in Supplementary Table 5.

### Co-immunoprecipitation

Protein lysates were incubated with 2 µg of antibody. After 4h rotation at 4°C, 20 µl of Protein A UltraLink Resin (Thermo Scientific, Waltham, MA, USA; 53139) was added for overnight incubation at 4°C. Beads were washed 3 times with RIPA buffer and immunoprecipitates were eluted by heating the beads at 95 °C in 2× SDS loading buffer (62 mM Tris–HCl (pH 6.8), 4% SDS, 20% glycerol, 0.01% BFB (bromophenol blue), 2.5% beta-mercaptoethanol) for 10 min. A part of the original lysates were similarly denaturated by heating at 95 °C for 10 min after adding 5× SDS loading buffer (155 mM Tris–HCl (pH 6.8), 5% SDS, 32% glycerol, 0.025% BFB, 2,5% beta mercapto-ethanol).

### Modulation of BIM expression

The pENTR223-BCL2L11 (LMBP ORF81079-A09) plasmid was available from the BCCM/LMBP Plasmid Collection(25) and was used to clone *BCL2L11* in the pInducer21 plasmid(26). The MISSION lentiviral shBCL2L11 TRCN0000001051 (Sigma-Aldrich) vector (BCCM/LMBP Collection (25)), in which the puromycin resistance cassette was replaced by eGFP, was used to perform BIM knockdown. As non-targeting shRNA control, MISSION pLKO.1-puro Non-Mammalian shRNA Control Plasmid (SHC002), in which also puro was replaced by eGFP, was used. Virus production was performed in HEK293TN cells using JetPEI polyplus with pMD2.G (envelope plasmid), psPAX2 (packaging plasmid) and target plasmid in 0.1/0.9/1 ratios. Transduced KARPAS-45 cells expressing GFP were selected by cell sorting. *BCL2L11* expression was induced by adding doxycyclin (1µg/ml) and sensitivity to venetoclax was evaluated by adding venetoclax together with or without doxycycline for 48h to the cells. To evaluate

the effect of BIM knockdown, cells were treated with venetoclax, JQ1 or the combination for 48h.

Viability was evaluated with CellTiter Glo as described above.

## Statistics

GraphPad Prism 5.04 (La Jolla, CA, USA) was used for statistical analyses.

## Results

### Identification of synergistic drug combinations with venetoclax in primary human T-ALL

Previous studies have shown promising anti-tumor activity for venetoclax in the context of human T-ALL(8-10). However, drug responses have been variable across patients both *in vitro* as well as in xenografts, suggesting the need for predictive biomarkers and further investigation towards synergistic drug combinations with venetoclax. Given this, we took advantage of a drug-profiling platform(27) (**Figure 1A**) to test 21 clinically relevant compounds (**Supplementary Table 1**) for their ability to synergize with venetoclax in six primary human T-ALLs, including five diagnostic and one relapse specimen. Notably, the selected patient samples represented different molecular genetic subtypes of human T-ALL and displayed a variety of tumor immunophenotypes. In addition, they displayed variable levels of BCL-2 and BIM protein expression (**Supplementary Figure 1A**) and most of these high-risk T-ALL patient samples experienced significant levels of minimal residual disease upon first line therapy (**Supplementary Table 2**).

First, we generated venetoclax response curves for each T-ALL sample and selected a sub-lethal dose of venetoclax for screening purposes (**Figure 1A**). Two T-ALL samples were sensitive at concentrations below 100nM, whereas the remaining cases were more resistant to venetoclax (**Supplementary Figure 1B**). This variability in venetoclax sensitivity amongst T-ALL patient samples corresponded to large differences in the area under the curve (AUC), a parameter that captures both  $IC_{50}$  and  $E_{max}$  as relevant endpoints of drug activity (**Figure 1B**). Next, we generated dose response curves (1nM, 10 nM, 100nM, 1 $\mu$ M and 10 $\mu$ M) for the 21 compounds in the presence or absence of a

sublethal dose of venetoclax (**Figure 1A**). The results of this initial screening are visualised by scatterplots of AUC values, in which decreased AUC upon addition of venetoclax is indicative of increased antileukemic activity (**Figure 1B**; **Supplementary Figure 2**). In line with previous studies, combination of venetoclax with conventional chemotherapeutic agents including vincristine, dexamethasone and etoposide increased therapeutic efficacy in some of the T-ALL cases analysed (**Figure 1B**). The strongest effects, however, were observed for the combination of venetoclax with JQ1, which resulted in reduced leukemic tumor growth in 5 out of 6 primary T-ALL patient samples (**Figure 1B**). As a confirmation, we validated responsive (**Figure 1C**) as well as non-responsive (**Supplementary Figure 3**) drug interactions identified in this initial screen. Altogether, this screening effort identified clinically relevant drugs that could increase the therapeutic efficacy of venetoclax in the context of T-ALL.

#### **Combined targeting of BCL-2 and BET bromodomain proteins in human T-ALL**

Given that our initial screen pointed towards increased efficacy of venetoclax upon BET bromodomain inhibition in a significant proportion of T-ALLs, we subsequently analysed the synergistic potential of this drug combination in more detail by performing co-titration experiments with individually-optimized concentration ranges in primary leukemias and a panel of human T-ALL cell lines.

First, we determined the combination indexes (CI) for the 6 primary T-ALLs that were also used for the initial screening and identified synergistic activities ( $CI < 1$ ) between venetoclax and JQ1 in five out of six cases analysed (**Figure 2A**). Notably, similar results were obtained using OTX015 (MK-8628), another BET bromodomain inhibitor currently being tested in clinical trials for various tumor entities(28, 29) (**Supplementary Figure 4**).

Next, we determined dose response curves in a panel of 13 human T-ALL cell lines with different BCL-2 levels and varying sensitivities towards venetoclax (**Figure 2B** and **Supplementary Figure 5**). Notably, T-ALL cell lines displayed variable levels of synergism with the lowest CI values (strongest

synergism) detected for tumor lines with high BCL-2 expression (**Figure 2B**). Indeed, the combination index showed a negative correlation with BCL-2 protein levels in T-ALL cell lines (**Figure 2C**). Moreover, synergistic activity of this drug combination corresponded to increased cell death induction in T-ALL cell lines with low CI values (**Supplementary Figure 6**).

### Evaluation of the venetoclax and JQ1 combination therapy in xenograft models

To evaluate the therapeutic potential of combined BCL-2 and BET bromodomain inhibition in human T-ALL, we subsequently performed *in vivo* drug treatment experiments using xenograft models. Four weeks after injection of luciferase-positive LOUCY cells(8) in immunodeficient mice, successful engraftment was confirmed by bioluminescence imaging and daily drug treatment was initiated (day 1-13). Leukemia still progressed under JQ1 monotherapy (n=5), albeit to a lesser extent as compared to vehicle-treated control mice (n=8) (**Figure 3A** and **Supplementary Figure 7**). Mice treated for 13 days with venetoclax alone (n=5) initially showed disease regression, but this therapeutic response was not durable (**Figure 3A** and **Supplementary Figure 7**). In contrast, combination of venetoclax with JQ1 (n=5) resulted in durable disease regression (**Figure 3A-B**). In line with these results, analysis of the percentage of human leukemic cells in peripheral blood and bone marrow as well as examination of the spleen size confirmed the superior therapeutic effect of this combination treatment (**Figure 3C-D** and **Supplementary Figure 8**). Of note, mice receiving JQ1 alone or in combination with venetoclax displayed significant weight loss (**Supplementary Figure 8**), a putative side effect of BET bromodomain inhibition. The synergistic effect of combined BCL-2 and BET bromodomain inhibition was also confirmed in the *TLX1* positive T-ALL cell line ALL-SIL (**Supplementary Figure 9**). The genetic characteristics of LOUCY and ALL-SIL are summarized in **Supplementary Table 3**.

Finally, we performed a similar *in vivo* drug treatment experiment using a primary patient-derived xenograft. For this, leukemic cells from the very high risk T-ALL patient (T-VHR-26) were engrafted and treated with a similar drug regimen as mentioned above. Notably, this experiment confirmed the

superior therapeutic effect of combined BCL-2 and BET bromodomain inhibition for the treatment of this high risk T-ALL patient sample (**Figure 4** and **Supplementary Figure 10**). Of note, in this experiment, no significant weight loss was observed in any of the treatment groups (**Supplementary Figure 10C**).

### **Mechanistic insights into the synergistic activities of venetoclax and JQ1 in human T-ALL**

To understand how BET bromodomain inhibition might synergize with the BCL-2 inhibitor venetoclax, we subsequently analyzed the transcriptional consequences of JQ1 treatment in the T-ALL cell line LOUCY by microarray analysis. Short-term exposure to a low dose of JQ1 (4h, 250nM) provided insights in the genes whose expression was immediately affected by BET bromodomain inhibition (**Figure 5A**, left). In contrast, sustained exposure at a higher concentration (48h, 1 $\mu$ M) revealed broader transcriptional effects with more than half of the expressed probesets showing significant up- or downregulation (adj. p-value<0.05; **Figure 5A**, right). Significantly downregulated genes upon short-term drug treatment included stem-cell associated genes and putative oncogenes such as *BAALC*, *WT1*, *MN1*, *MEF2C*, *LMO1* and *LMO2*, whereas other oncogenic factors, including *BCL2*, *IGFBP7*, *ZEB2*, *GFI1B*, *MYB* and *LYL1*, only changed significantly after 48h.

In line with previous reports(17-19), these JQ1 responsive genes were regulated by strong and active enhancer elements characterized by broad binding of the H3K27ac histone mark in LOUCY cells(30) (**Figure 5B**). Indeed, genes associated with the 500 highest ranked enhancer regions in LOUCY were significantly enriched in genes downregulated after JQ1 treatment (**Figure 5C**). Moreover, enrichment analysis using gene sets from the Molecular Signatures database (MSigDB) revealed that genes upregulated after JQ1 in LOUCY cells significantly overlapped with genes activated upon HDAC inhibition (**Figure 5D**). In line with this notion, the Library of Integrated Cellular Signatures (LINCS) revealed a strong connection between the JQ1-induced expression signature in LOUCY and gene signatures induced by HDAC inhibitors (**Supplementary Table 4**).

Given that binding of the pro-apoptotic BIM (encoded by *BCL2L11*) to the BH3 domain of BCL-2 is an important mediator of venetoclax activity(31-34), we subsequently focused on the transcriptional effects of JQ1 on the expression of both factors. Notably, in LOUCY cells, *BCL2L11* expression was induced after short-term JQ1 exposure (**Figure 5A**, left), whereas loss of *BCL2* expression was only detected at later time points (**Figure 5A**, right). In addition, the expression of the miR17-92 cluster, a known negative regulator of BIM(35) was not affected after 4h of JQ1 treatment but was clearly downregulated after 48h (**Supplementary Figure 11A**). Upregulation of pro-apoptotic *BCL2L11* and concomitant loss of anti-apoptotic *BCL-2* could be confirmed in all T-ALL cell lines that displayed strong synergy ( $CI < 0.5$ ) for the ABT199/JQ1 drug combination. As a result, BET bromodomain inhibition triggered an increased BIM to BCL-2 ratio (**Figure 6A and Supplementary Figure 11B**), providing a putative explanation for the improved therapeutic efficacy of venetoclax upon JQ1 treatment. Indeed, co-immunoprecipitation experiments demonstrated an increased BIM to BCL-2 binding (**Figure 6B**) upon JQ1 treatment. Finally, doxycycline inducible overexpression of BIM in the KARPAS-45 cell line mimicked the effect of JQ1 and resulted in an increased sensitivity towards venetoclax (**Figure 6C**) while knockdown of BIM lowered the sensitivity to ABT-199, JQ1 and combination treatment (**Figure 6D**).

## Discussion

Venetoclax is a promising new molecular therapy that is currently being evaluated in clinical trials for different hematological malignancies(14, 15, 36). However, the limited number of complete remissions(14) and the emergence of resistance with venetoclax as single agent prompts for a systematic evaluation of combinations with rationally-designed small molecules to assess its true therapeutic potential. Indeed, synergistic cytotoxic effects have been described for the combination of venetoclax with BTK(37-39), galectin(40), Aurora Kinase A(41), CDK(42, 43) and PI3K/AKT/mTOR inhibition(13, 44).



Given the promising single agent activity of venetoclax in human T-ALL subsets(8-10), we systematically evaluated clinically relevant drugs in order to identify synergistic combinations with venetoclax. The strongest and most consistent effect was detected for the combination with the bromodomain inhibitors JQ1 and OTX015, both targeting critical mechanisms that are deregulated in cancer cells. This effect could be validated *in vivo* using leukemia xenograft models. Notably, this concept has recently been suggested as an experimental therapy for double hit lymphoma, triple hit lymphoma and mantle cell lymphoma in which both *MYC* and *BCL2* are deregulated(45-47). Interestingly, our preclinical data indicate that relevant activity can be obtained with this combination of agents irrespectively from their activity as single agent, which may possibly broaden the cohort of eligible cancer types (or subsets) for clinical translation. However, the challenge will be to identify useful biomarkers to better define patients that may benefit from such experimental combinations. Interestingly, an increase of BCL-2 protein levels in human T-ALL cell lines correlated with synergism between venetoclax and JQ1. Nevertheless, the value of additional methodologies such as BH3-profiling(48) should also be taken into consideration in future studies of this therapeutic rationale.

The importance of BRD4 in processes that lead to abnormal activation of cancer driving genetic programs is increasingly being understood(17-19). The proof of concept in T-ALL was provided by studies of BET bromodomain inhibitors with a focus on *MYC* inhibition(20-22). Given the central importance of super-enhancer deregulation in cancer(18, 19), a similar principle may apply to many different transcriptional programs in leukemia cells. However, the broad transcriptional effects of these inhibitors on T-ALL cells remain largely unexplored. Gene expression profiling of LOUCY cells treated with JQ1 confirmed that BET bromodomain inhibition results in reduced expression of super-enhancer-associated oncogenes as previously described by Lovén et al.(17). Similar effects have also previously been reported for the T-ALL cell line ALL-SIL(49). Although there is some overlap between super-enhancers in different T-ALL cell lines(18, 49), each cell line seems to have a pretty unique spectrum of super-enhancer sequences. However, we also observed acute gene activation within 4

hours of JQ1 treatment. In the gene signature that was activated upon JQ1 treatment in LOUCY cells, HDACi associated gene sets were enriched. This is in accordance with Bhadury et al.(50) who describe a large overlap between genes induced by BETi and HDACi.

*BCL2L11* (encoding BIM) is one of the genes that showed such an acute induction of gene expression upon JQ1 treatment in the context of T-ALL. BIM is an activator BH3-only pro-apoptotic protein that can directly interact with BAX and/or BAK to induce apoptosis. BCL-2 can prevent apoptosis by sequestering pro-apoptotic proteins such as BIM(51). Studies demonstrated the requirement for BCL-2 complexed to the pro-apoptotic activator BIM in order to sensitize lymphoid cells to BCL-2 inhibition by venetoclax or ABT-737(31-34). In our study, BET bromodomain inhibition increased BIM to BCL-2 binding, and could provide a putative explanation for the observed synergism between venetoclax and JQ1/OTX015 in the context of human T-ALL. Importantly, upregulation of pro-apoptotic BIM upon JQ1 treatment has also been described in a variety of other tumor entities(52-55), suggesting that the synergistic activity between these molecules might not be restricted to human T-ALL. Xu et al.(56) attributed the upregulation of *BCL2L11* in response to JQ1 to the downregulation of the miR17-92 cluster. We also observed a downregulation of the miR17-92 cluster but not yet after 4h of JQ1 treatment, a timepoint with already significant upregulation of *BCL2L11* in LOUCY. Therefore, this mechanism does not explain the acute upregulation of *BCL2L11* but this could definitely contribute to sustain the upregulation of *BCL2L11*.

In summary, our study provides a rationale to select patients with treatment resistant T-ALL for an innovative combination treatment based on mechanisms that are not exploited by conventional chemotherapy regimens. Interference with the balance between pro- and anti-apoptotic proteins in BCL2-dependent T-ALL using the combination BET bromodomain inhibition and the BCL2-inhibitor venetoclax should be considered in future clinical trials for this indication.

## Acknowledgments

The authors would like to thank following funding agencies: Fund for Scientific Research Flanders ('FWO Vlaanderen' research projects GA00113N, 3G065614, G.0C47.13N and 31500615W to PVV; research projects G.0529.12N and G.0817.13N to GB; doctoral grant to SP; postdoctoral grant to SG; BP is a senior clinical investigator), Children Cancer Fund Ghent, Belgian Foundation Against Cancer (grant 365W3415W and B/13590) and the Belgian Stand Up To Cancer Foundation (research grant 365Y9115W; doctoral grant to SP; postdoctoral grants to TP and FM), agency for Innovation by Science and Technology ('IWT', SB Grant 111528 to NV), Geconcerteerde Onderzoeksacties Ghent University (GOA-01GB1013W to GB), Cancer League of the Canton of Zurich, Empiris Foundation, Kinderkrebsforschung Schweiz, Sassella Foundation, Stiftung für Krebsbekämpfung, Swiss National Science Foundation (310030-133108), Fondation Panacée and the clinical research focus program "Human Hemato-Lymphatic Diseases" of the University of Zurich.

The authors also thank Lindy Reunes for excellent technical assistance and the Innovative Flemish in vivo imaging technology (INFINITY) laboratory at Ghent University Hospital. Finally, the computational resources (Stevin Supercomputer Infrastructure) and services used in this work were provided by the VSC (Flemish Supercomputer Center), funded by Ghent University, the Hercules Foundation and the Flemish Government – department EWI.

## Conflict of Interest

The authors declare no conflict of interest.

Supplementary information is available at Leukemia's website.

## References

1. Pui C-H, Relling MV, Downing JR. Acute Lymphoblastic Leukemia. *N Engl J Med*. 2004;350(15):1535-48.
2. Pui CH, Pei D, Campana D, Cheng C, Sandlund JT, Bowman WP, et al. A revised definition for cure of childhood acute lymphoblastic leukemia. *Leukemia*. 2014;28(12):2336-43.
3. Pui CH, Mullighan CG, Evans WE, Relling MV. Pediatric acute lymphoblastic leukemia: where are we going and how do we get there? *Blood*. 2012;120(6):1165-74.
4. Bhojwani D, Pui CH. Relapsed childhood acute lymphoblastic leukaemia. *Lancet Oncol*. 2013;14(6):e205-17.
5. Bassan R, Hoelzer D. Modern therapy of acute lymphoblastic leukemia. *J Clin Oncol*. 2011;29(5):532-43.
6. Oriol A, Vives S, Hernandez-Rivas JM, Tormo M, Heras I, Rivas C, et al. Outcome after relapse of acute lymphoblastic leukemia in adult patients included in four consecutive risk-adapted trials by the PETHEMA Study Group. *Haematologica*. 2010;95(4):589-96.
7. Faderl S, O'Brien S, Pui CH, Stock W, Wetzler M, Hoelzer D, et al. Adult acute lymphoblastic leukemia: concepts and strategies. *Cancer*. 2010;116(5):1165-76.
8. Peirs S, Matthijssens F, Goossens S, Van de Walle I, Ruggero K, de Bock CE, et al. ABT-199 mediated inhibition of BCL-2 as a novel therapeutic strategy in T-cell acute lymphoblastic leukemia. *Blood*. 2014;124(25):3738-47.
9. Anderson NM, Harrold I, Mansour MR, Sanda T, McKeown M, Nagykaray N, et al. BCL2-specific inhibitor ABT-199 synergizes strongly with cytarabine against the early immature LOUCY cell line but not more-differentiated T-ALL cell lines. *Leukemia*. 2014;28(5):1145-8.
10. Chonghaile TN, Roderick JE, Glenfield C, Ryan J, Sallan SE, Silverman LB, et al. Maturation Stage of T-cell Acute Lymphoblastic Leukemia Determines BCL-2 versus BCL-XL Dependence and Sensitivity to ABT-199. *Cancer discovery*. 2014.

11. Fresquet V, Rieger M, Carolis C, Garcia-Barchino MJ, Martinez-Climent JA. Acquired mutations in BCL2 family proteins conferring resistance to the BH3 mimetic ABT-199 in lymphoma. *Blood*. 2014;123(26):4111-9.
12. Tahir SK, Smith ML, Hessler P, Roberts-Rapp L, Levenson JD, Lam LT. Abstract B30: Mechanisms of resistance to ABT-199 in leukemia and lymphoma cell lines. *Clin Cancer Res*. 2015;21(4 Supplement):B30.
13. Choudhary GS, Al-Harbi S, Mazumder S, Hill BT, Smith MR, Bodo J, et al. MCL-1 and BCL-xL-dependent resistance to the BCL-2 inhibitor ABT-199 can be overcome by preventing PI3K/AKT/mTOR activation in lymphoid malignancies. *Cell death & disease*. 2015;6:e1593.
14. Roberts AW, Davids MS, Pagel JM, Kahl BS, Puvvada SD, Gerecitano JF, et al. Targeting BCL2 with Venetoclax in Relapsed Chronic Lymphocytic Leukemia. *N Engl J Med*. 2016;374(4):311-22.
15. Stilgenbauer S, Eichhorst B, Schetelig J, Coutre S, Seymour JF, Munir T, et al. Venetoclax in relapsed or refractory chronic lymphocytic leukaemia with 17p deletion: a multicentre, open-label, phase 2 study. *The Lancet Oncology*. 2016.
16. Filippakopoulos P, Qi J, Picaud S, Shen Y, Smith WB, Fedorov O, et al. Selective inhibition of BET bromodomains. *Nature*. 2010;468(7327):1067-73.
17. Loven J, Hoke HA, Lin CY, Lau A, Orlando DA, Vakoc CR, et al. Selective inhibition of tumor oncogenes by disruption of super-enhancers. *Cell*. 2013;153(2):320-34.
18. Hnisz D, Abraham BJ, Lee TI, Lau A, Saint-Andre V, Sigova AA, et al. Super-enhancers in the control of cell identity and disease. *Cell*. 2013;155(4):934-47.
19. Filippakopoulos P, Knapp S. Targeting bromodomains: epigenetic readers of lysine acetylation. *Nat Rev Drug Discov*. 2014;13(5):337-56.
20. Loosveld M, Castellano R, Gon S, Goubard A, Crouzet T, Pouyet L, et al. Therapeutic targeting of c-Myc in T-cell acute lymphoblastic leukemia, T-ALL. *Oncotarget*. 2014;5(10):3168-72.

21. Roderick JE, Tesell J, Shultz LD, Brehm MA, Greiner DL, Harris MH, et al. c-Myc inhibition prevents leukemia initiation in mice and impairs the growth of relapsed and induction failure pediatric T-ALL cells. *Blood*. 2014;123(7):1040-50.
22. King B, Trimarchi T, Reavie L, Xu L, Mullenders J, Ntziachristos P, et al. The ubiquitin ligase FBXW7 modulates leukemia-initiating cell activity by regulating MYC stability. *Cell*. 2013;153(7):1552-66.
23. Bonapace L, Bornhauser BC, Schmitz M, Cario G, Ziegler U, Niggli FK, et al. Induction of autophagy-dependent necroptosis is required for childhood acute lymphoblastic leukemia cells to overcome glucocorticoid resistance. *J Clin Invest*. 2010;120(4):1310-23.
24. Edgar R, Domrachev M, Lash AE. Gene Expression Omnibus: NCBI gene expression and hybridization array data repository. *Nucleic Acids Res*. 2002;30(1):207-10.
25. Yang X, Boehm JS, Yang X, Salehi-Ashtiani K, Hao T, Shen Y, et al. A public genome-scale lentiviral expression library of human ORFs. *Nat Methods*. 2011;8(8):659-61.
26. Meerbrey KL, Hu G, Kessler JD, Roarty K, Li MZ, Fang JE, et al. The pINDUCER lentiviral toolkit for inducible RNA interference in vitro and in vivo. *Proc Natl Acad Sci U S A*. 2011;108(9):3665-70.
27. Fischer U, Forster M, Rinaldi A, Risch T, Sungalee S, Warnatz HJ, et al. Genomics and drug profiling of fatal TCF3-HLF-positive acute lymphoblastic leukemia identifies recurrent mutation patterns and therapeutic options. *Nat Genet*. 2015;47(9):1020-9.
28. Berthon C, Raffoux E, Thomas X, Vey N, Gomez-Roca C, Yee K, et al. Bromodomain inhibitor OTX015 in patients with acute leukaemia: a dose-escalation, phase 1 study. *Lancet Haematol*. 2016;3(4):e186-95.
29. Amorim S, Stathis A, Gleeson M, Iyengar S, Magarotto V, Leleu X, et al. Bromodomain inhibitor OTX015 in patients with lymphoma or multiple myeloma: a dose-escalation, open-label, pharmacokinetic, phase 1 study. *Lancet Haematol*. 2016;3(4):e196-204.

30. Wallaert A, Durinck K, Van Loocke W, Van de Walle I, Matthijssens F, Volders PJ, et al. Long noncoding RNA signatures define oncogenic subtypes in T-cell acute lymphoblastic leukemia. *Leukemia*. 2016.
31. Souers AJ, Levenson JD, Boghaert ER, Ackler SL, Catron ND, Chen J, et al. ABT-199, a potent and selective BCL-2 inhibitor, achieves antitumor activity while sparing platelets. *Nat Med*. 2013;19(2):202-8.
32. Del Gaizo Moore V, Brown JR, Certo M, Love TM, Novina CD, Letai A. Chronic lymphocytic leukemia requires BCL2 to sequester prodeath BIM, explaining sensitivity to BCL2 antagonist ABT-737. *J Clin Invest*. 2007;117(1):112-21.
33. Merino D, Khaw SL, Glaser SP, Anderson DJ, Belmont LD, Wong C, et al. Bcl-2, Bcl-x(L), and Bcl-w are not equivalent targets of ABT-737 and navitoclax (ABT-263) in lymphoid and leukemic cells. *Blood*. 2012;119(24):5807-16.
34. Khaw SL, Merino D, Anderson MA, Glaser SP, Bouillet P, Roberts AW, et al. Both leukaemic and normal peripheral B lymphoid cells are highly sensitive to the selective pharmacological inhibition of prosurvival Bcl-2 with ABT-199. *Leukemia*. 2014;28(6):1207-15.
35. Mogilyansky E, Rigoutsos I. The miR-17/92 cluster: a comprehensive update on its genomics, genetics, functions and increasingly important and numerous roles in health and disease. *Cell Death Differ*. 2013;20(12):1603-14.
36. Cang S, Iragavarapu C, Savooji J, Song Y, Liu D. ABT-199 (venetoclax) and BCL-2 inhibitors in clinical development. *J Hematol Oncol*. 2015;8:129.
37. Cervantes-Gomez F, Lamothe B, Woyach JA, Wierda WG, Keating MJ, Balakrishnan K, et al. Pharmacological and Protein Profiling Suggests Venetoclax (ABT-199) as Optimal Partner with Ibrutinib in Chronic Lymphocytic Leukemia. *Clin Cancer Res*. 2015;21(16):3705-15.
38. Chiron D, Dousset C, Brosseau C, Touzeau C, Maiga S, Moreau P, et al. Biological rationale for sequential targeting of Bruton tyrosine kinase and Bcl-2 to overcome CD40-induced ABT-199 resistance in mantle cell lymphoma. *Oncotarget*. 2015;6(11):8750-9.

39. Zhao X, Bodo J, Sun D, Durkin L, Lin J, Smith MR, et al. Combination of ibrutinib with ABT-199: synergistic effects on proliferation inhibition and apoptosis in mantle cell lymphoma cells through perturbation of BTK, AKT and BCL2 pathways. *Br J Haematol*. 2015;168(5):765-8.
40. Ruvolo PP, Ruvolo VR, Benton CB, AlRawi A, Burks JK, Schober W, et al. Combination of galectin inhibitor GCS-100 and BH3 mimetics eliminates both p53 wild type and p53 null AML cells. *Biochim Biophys Acta*. 2016;1863(4):562-71.
41. Ham J, Costa C, Sano R, Lochmann TL, Sennott EM, Patel NU, et al. Exploitation of the Apoptosis-Primed State of MYCN-Amplified Neuroblastoma to Develop a Potent and Specific Targeted Therapy Combination. *Cancer Cell*. 2016;29(2):159-72.
42. Phillips DC, Xiao Y, Lam LT, Litvinovich E, Roberts-Rapp L, Souers AJ, et al. Loss in MCL-1 function sensitizes non-Hodgkin's lymphoma cell lines to the BCL-2-selective inhibitor venetoclax (ABT-199). *Blood Cancer J*. 2015;5:e368.
43. Choudhary GS, Tat TT, Misra S, Hill BT, Smith MR, Almasan A, et al. Cyclin E/Cdk2-dependent phosphorylation of Mcl-1 determines its stability and cellular sensitivity to BH3 mimetics. *Oncotarget*. 2015;6(19):16912-25.
44. Lee JS, Tang SS, Ortiz V, Vo TT, Fruman DA. MCL-1-independent mechanisms of synergy between dual PI3K/mTOR and BCL-2 inhibition in diffuse large B cell lymphoma. *Oncotarget*. 2015;6(34):35202-17.
45. Sun B, Shah B, Fiskus W, Qi J, Rajapakshe K, Coarfa C, et al. Synergistic activity of BET protein antagonist-based combinations in mantle cell lymphoma cells sensitive or resistant to ibrutinib. *Blood*. 2015;126(13):1565-74.
46. Cinar M, Rosenfelt F, Rokhsar S, Lopategui J, Pillai R, Cervania M, et al. Concurrent inhibition of MYC and BCL2 is a potentially effective treatment strategy for double hit and triple hit B-cell lymphomas. *Leuk Res*. 2015;39(7):730-8.



47. Johnson-Farley N, Veliz J, Bhagavathi S, Bertino JR. ABT-199, a BH3 mimetic that specifically targets Bcl-2, enhances the antitumor activity of chemotherapy, bortezomib and JQ1 in "double hit" lymphoma cells. *Leuk Lymphoma*. 2015;56(7):2146-52.
48. Certo M, Del Gaizo Moore V, Nishino M, Wei G, Korsmeyer S, Armstrong SA, et al. Mitochondria primed by death signals determine cellular addiction to antiapoptotic BCL-2 family members. *Cancer Cell*. 2006;9(5):351-65.
49. Durinck K, Van Looche W, Van der Meulen J, Van de Walle I, Ongenaert M, Rondou P, et al. Characterization of the genome-wide TLX1 binding profile in T-cell acute lymphoblastic leukemia. *Leukemia*. 2015;29(12):2317-27.
50. Bhadury J, Nilsson LM, Muralidharan SV, Green LC, Li Z, Gesner EM, et al. BET and HDAC inhibitors induce similar genes and biological effects and synergize to kill in Myc-induced murine lymphoma. *Proc Natl Acad Sci U S A*. 2014;111(26):E2721-30.
51. Hata AN, Engelman JA, Faber AC. The BCL2 Family: Key Mediators of the Apoptotic Response to Targeted Anticancer Therapeutics. *Cancer discovery*. 2015;5(5):475-87.
52. Sun B, Shah B, Fiskus W, Qi J, Rajapakshe K, Coarfa C, et al. Synergistic activity of BET protein antagonist-based combinations in mantle cell lymphoma cells sensitive or resistant to ibrutinib. *Blood*. 2015.
53. Tinsley S, Meja K, Shepherd C, Khwaja A. Synergistic induction of cell death in haematological malignancies by combined phosphoinositide-3-kinase and BET bromodomain inhibition. *Br J Haematol*. 2015;170(2):275-8.
54. Patel AJ, Liao CP, Chen Z, Liu C, Wang Y, Le LQ. BET bromodomain inhibition triggers apoptosis of NF1-associated malignant peripheral nerve sheath tumors through Bim induction. *Cell reports*. 2014;6(1):81-92.
55. Li GQ, Guo WZ, Zhang Y, Seng JJ, Zhang HP, Ma XX, et al. Suppression of BRD4 inhibits human hepatocellular carcinoma by repressing MYC and enhancing BIM expression. *Oncotarget*. 2016;7(3):2462-74.

56. Xu Z, Sharp PP, Yao Y, Segal D, Ang CH, Khaw SL, et al. BET inhibition represses miR17-92 to drive BIM-initiated apoptosis of normal and transformed hematopoietic cells. *Leukemia*. 2016;30(7):1531-41.

Accepted manuscript

## Figure Legends

**Figure 1 Drug-screening platform to identify novel synergistic combinations of venetoclax and other drugs**

- (A)** In a panel of primary T-ALL samples the effect of venetoclax treatment on cell viability was measured by flow cytometry using 7-AAD 72 hours after venetoclax treatment. Six representative samples (blue curves: sensitive to venetoclax; red curves: more resistant to venetoclax) were selected. For each sample, an optimal sub-lethal dose of venetoclax was calculated based on area under the curve (AUC) calculations of venetoclax as single agent. A single venetoclax dose was combined with selected clinically relevant compounds and the response change was compared to the control plate. Promising single compound combinations were validated in co-titration experiments.
- (B)** (i.) Scatterplots representing response of T-ALL samples (N=6) to venetoclax alone, shown as area under the curve (AUC). (ii.) Responses of T-ALL patient samples to combination of a sub-lethal venetoclax dose and indicated chemotherapeutic agents. AUC values of dose response curves from individual drug treatments (circles) or combined with venetoclax (triangles) are shown.
- (C)** Representative examples of co-titration assays for compounds found to synergize with venetoclax in preselected T-ALL samples from initial combination screening. (i) topoisomerase I inhibitor topotecan, (ii) dual PI3K and mTOR inhibitor dactolosib and (iii) BRD4 inhibitor JQ1.

**Figure 2 *In vitro* synergism between venetoclax and JQ1 in primary patient samples and T-ALL cell lines**

- (A)** Dose response curves are given for co-titration assays in primary T-ALL samples with increasing concentrations of both venetoclax and the BRD4 inhibitor JQ1. Combination

indices (CIs) indicate synergism for five of the six cases, and additive activity for the remaining sample.

- (B)** Overview of CIs between venetoclax and JQ1 in a panel of human T-ALL cell lines with indication of the degree of synergism. Mean and standard deviation of at least three independent experiments per cell line are represented. Western blot (bottom panel) indicates the BCL-2 protein levels in this cell line panel with  $\beta$ -actin as loading control.
- (C)** Scatterplot demonstrating the correlation between BCL-2 protein level and CI in the T-ALL cell lines.

**Figure 3 Combination treatment of mice xenografted with luciferase-positive human LOUCY cells**

- (A)** Leukemic burden was followed during the experiment on the basis of the luminescence of the leukemia cells. For each treatment group, one mouse is represented from day 0 (i.e. the day before the treatment started) till day 14 (i.e. the end of the experiment). The graph shows the average and standard deviation of the total flux of luminescence for all the mice in the group relative to the signal on day 0.
- (B)** Total flux of each mouse within a treatment group on day 14 relative to day 0.
- (C)** Percentage of hCD45+ leukemic cells in the peripheral blood for each mouse. All viable cells after red blood cell lysis were selected based on the forward and side scatter parameters. One sample from the control group could not be analyzed correctly.
- (D)** Percentage of hCD45+ leukemic cells in the bone marrow for each mouse. All the viable cells after red blood cell lysis were selected based on the forward and side scatter parameters.

The one-tailed Mann-Whitney test was used to compare the treatment groups statistically. ns not significant, \*  $P < 0.05$ , \*\*  $P < 0.01$ , \*\*\*  $P < 0.001$ . Horizontal lines on the graph indicate the median for each group.

**Figure 4 Combination treatment of patient (T-VHR-26)-derived xenograft**

- (A) Percentage of hCD45+ leukemic cells in the peripheral blood for each mouse after 14 days of treatment
- (B) Percentage of hCD45+ leukemic cells in the bone marrow for each mouse after 14 days of treatment
- (C) Percentage of hCD45+ leukemic cells in the liver for each mouse after 14 days of treatment

The one-tailed Mann-Whitney test was used to compare the treatment groups statistically. ns not significant, \*  $P < 0.05$ , \*\*  $P < 0.01$ , \*\*\*  $P < 0.001$ . Horizontal lines on the graph indicate the median for each group.

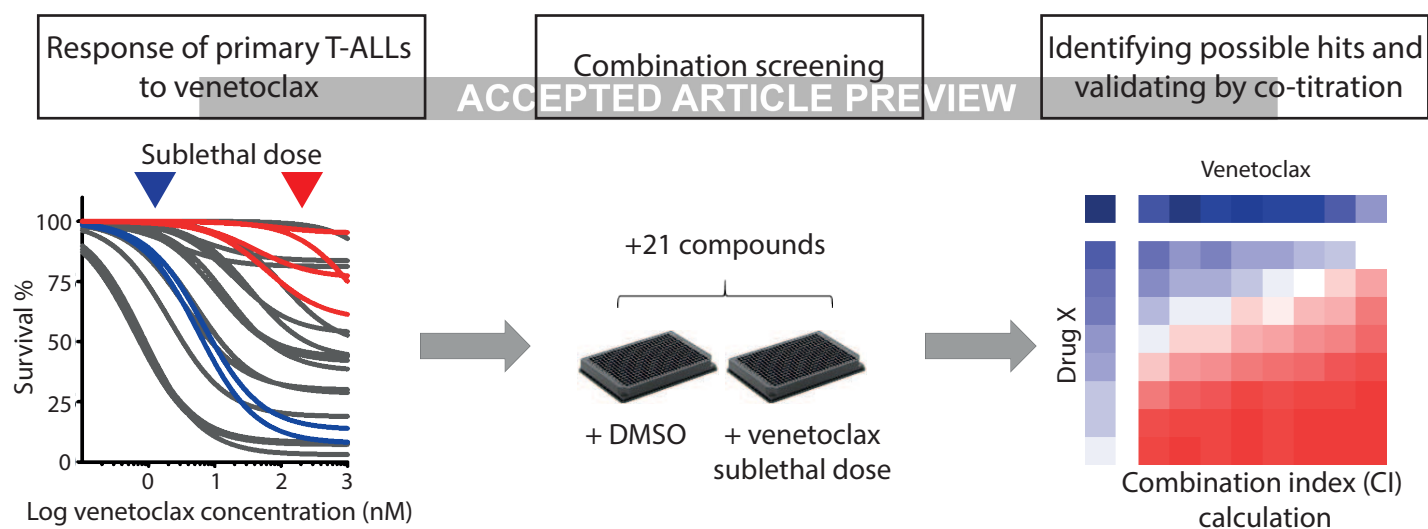
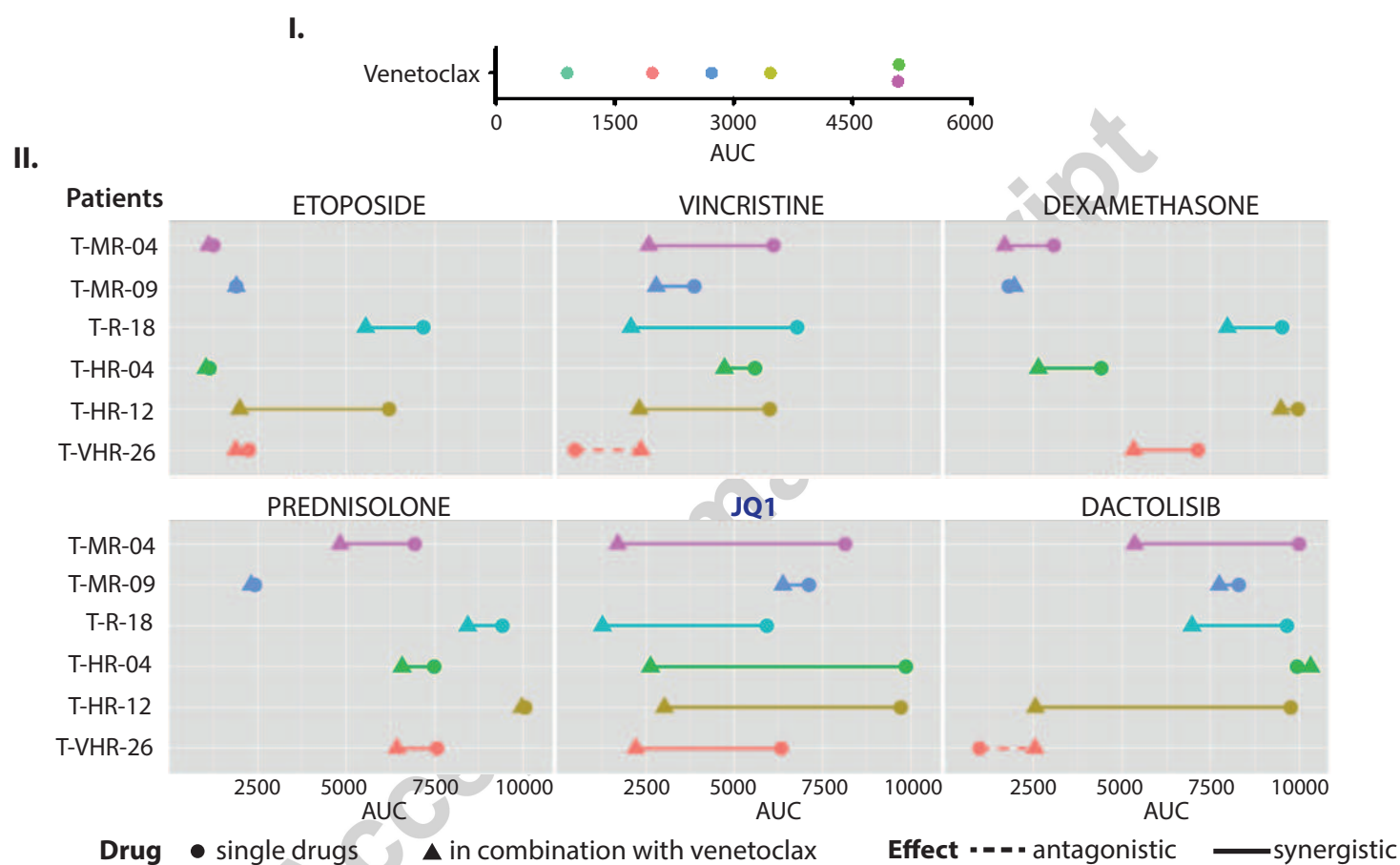
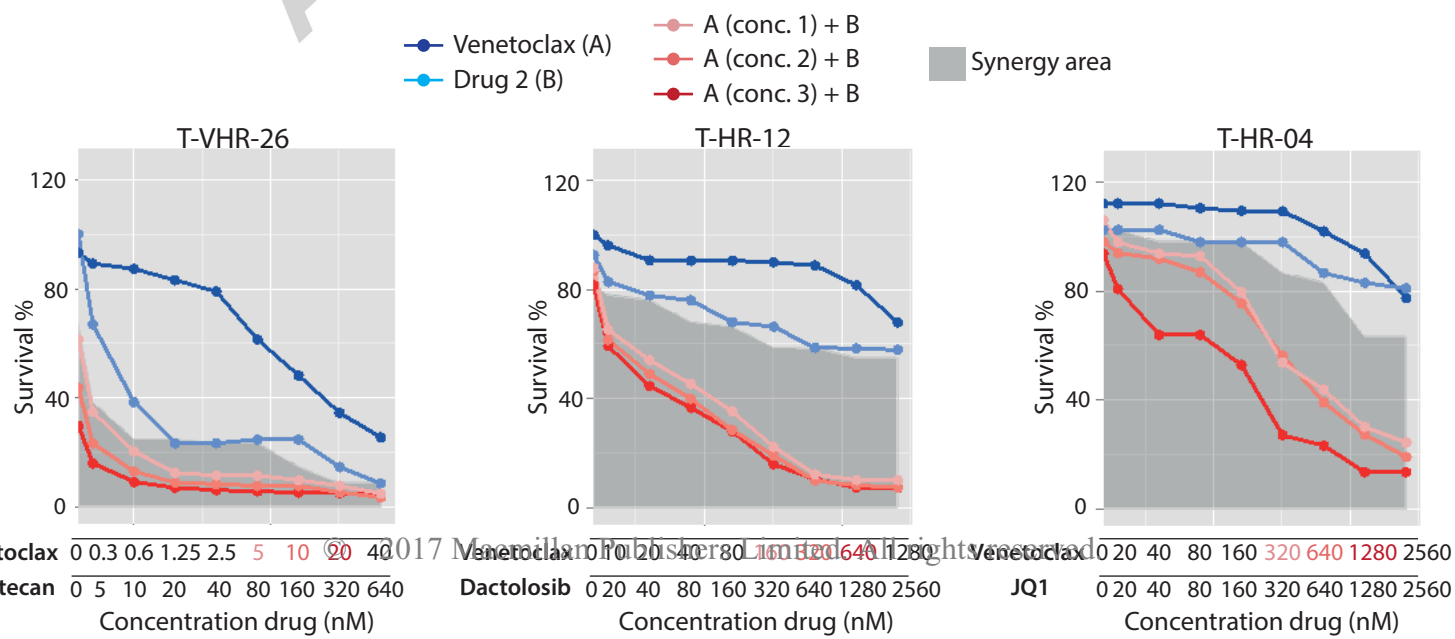
**Figure 5 Transcriptional effects of JQ1 on LOUCY**

- (A) Volcano plots displaying the differentially expressed genes in LOUCY after 4h of treatment with 250nM JQ1 (left) and 48h of treatment with 1 $\mu$ M JQ1 (right). In case multiple probes for one gene were present on the array, the differentially expressed probe with largest fold change was plotted.
- (B) Hockey-stick plot showing the ranked H3K27Ac-seq signal of all enhancers in LOUCY. Super-enhancers are indicated with blue dots. The red dots are examples of enhancers associated with interesting downregulated genes upon JQ1 treatment.
- (C) GSEA showing a significant enrichment of the genes associated with the top 500 super-enhancers in LOUCY among the downregulated genes after treatment with 250nM JQ1 for 4h (top) or 1 $\mu$ M JQ1 for 48h (bottom). The nearest TSS to each super-enhancer was determined via Peak Analyzer (OriginLab). This list of super-enhancer-associated genes was then used as a gene set for GSEA.
- (D) GSEA showing a significant enrichment of gene sets containing upregulated genes after HDACi among the upregulated genes after treatment of LOUCY with 250nM JQ1 for 4h. Left: DALESSIO\_TSA\_RESPONSE, i.e. top genes up-regulated in HEK293 cells in response to

trichostatin A (TSA). Right: PEART\_HDAC\_PROLIFERATION\_CLUSTER\_UP, i.e. cell proliferation genes up-regulated by histone deacetylase (HDAC) inhibitors SAHA and depsipeptide.

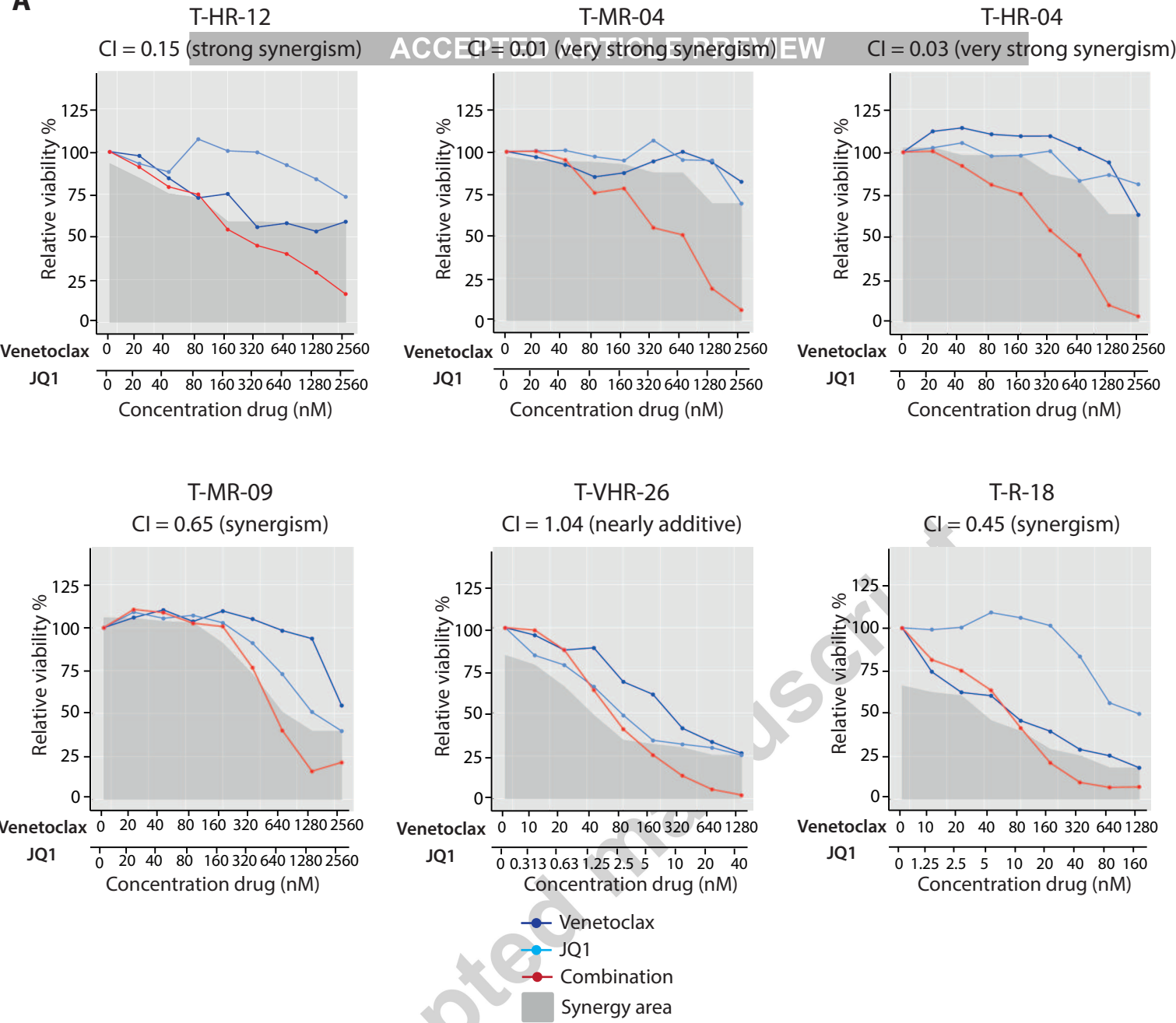
**Figure 6 Molecular insights in the mechanism of synergism**

- (A)** Western blot showing the increase of the BIM/BCL-2 protein ratio in synergistic T-ALL cell lines upon treatment with 1 $\mu$ M JQ1 for 48h. Only the upper band of BIM was quantified.
- (B)** Immunoprecipitation with anti-BIM antibody illustrates the increased binding of BIM to BCL-2 after JQ1 treatment.
- (C)** Induction of BIM expression in KARPAS-45 pInducer21-BCL2L11 cells increases the sensitivity to venetoclax. The average and stdev from 3 independent experiments is plotted. Western blot shows BIM induction for 3 independent replicates. The doublet seen for BIM<sub>EL</sub> (largest isoform) may represent phosphorylation.
- (D)** Knockdown of BIM in KARPAS-45 affects sensitivity to venetoclax, JQ1 and combination treatment. The average and stdev from 2 independent experiments is plotted. Western blot shows knockdown of BIM in the cells.

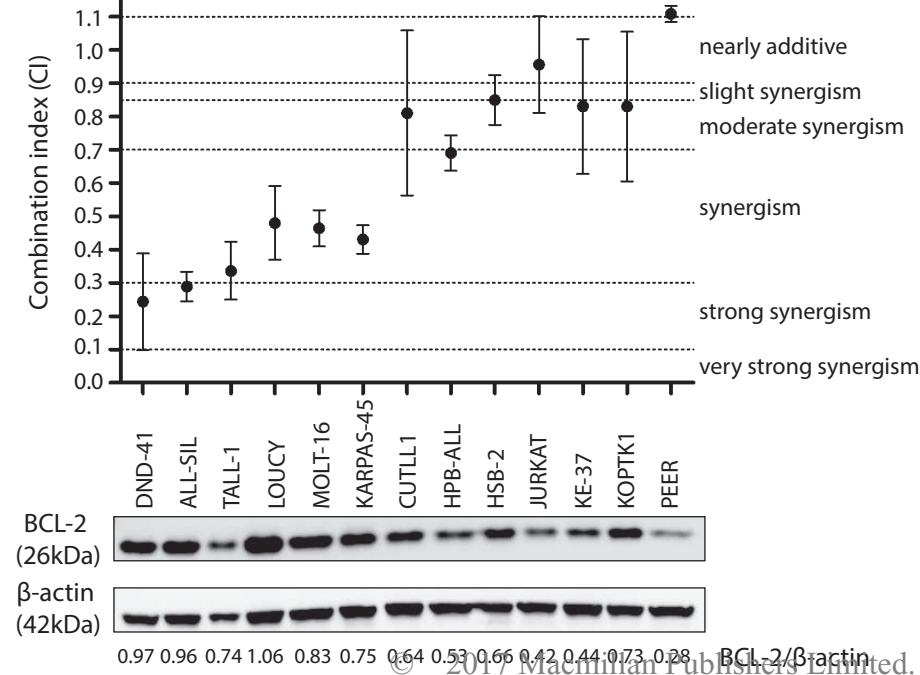
**Figure 1****A****B****C**

**Figure 2**

**A**



**B**



**C**

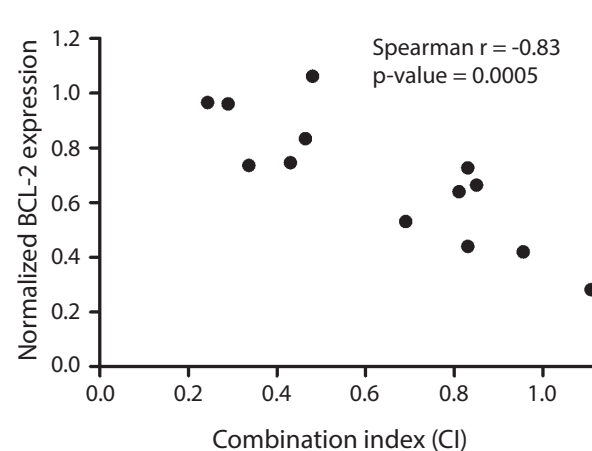
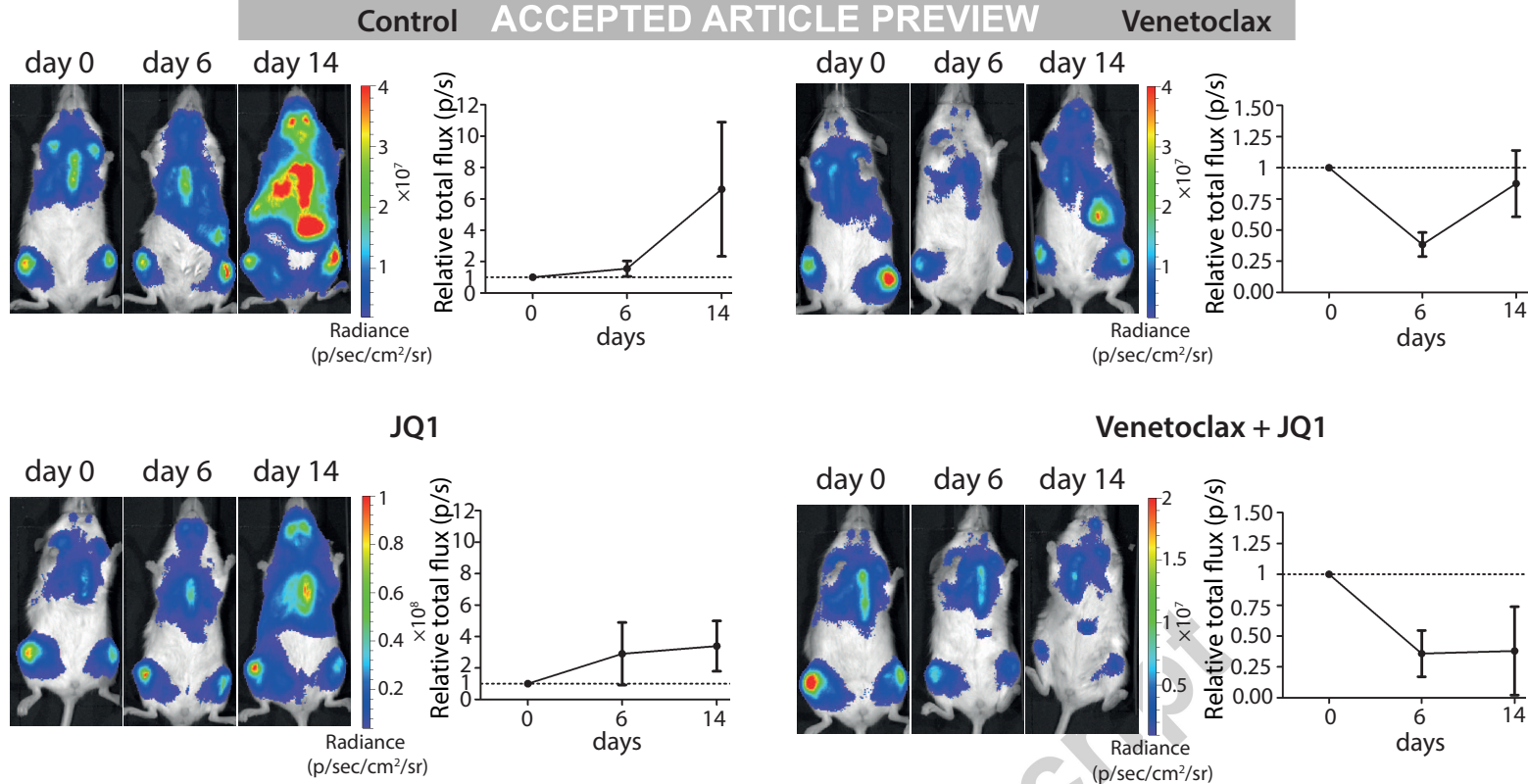


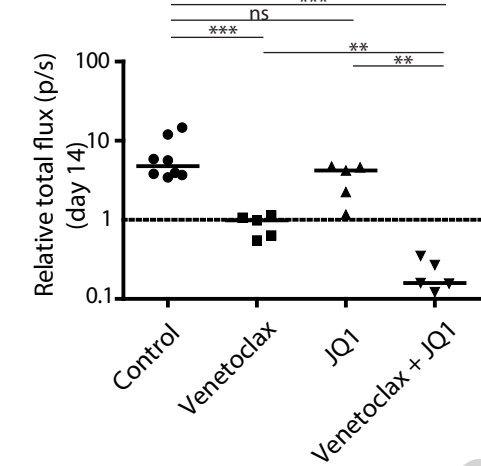


Figure 3

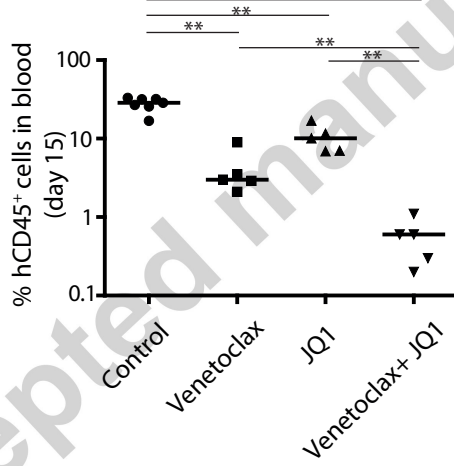
A



B



C



D

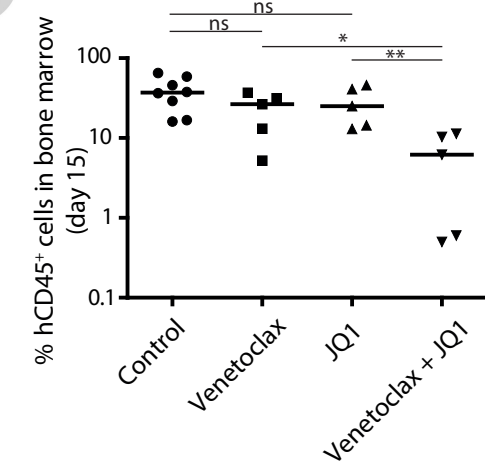
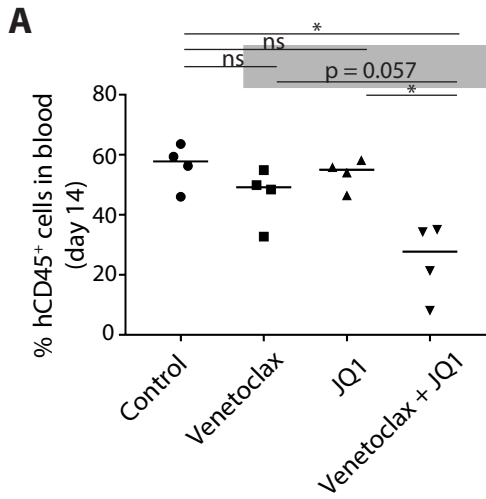
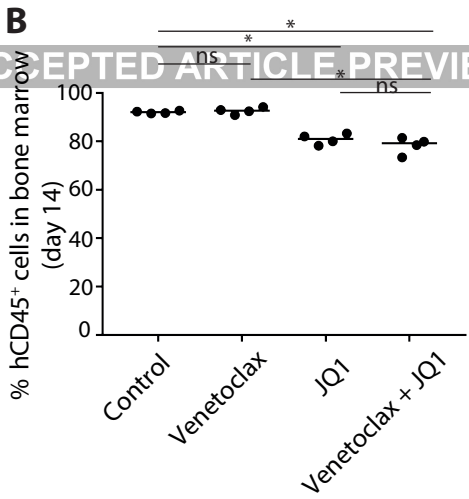


Figure 4

A



B



C

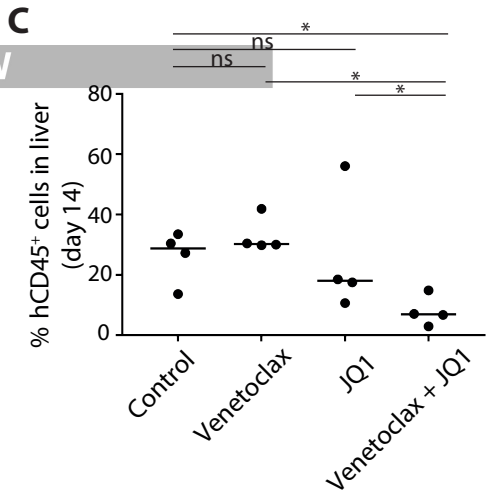
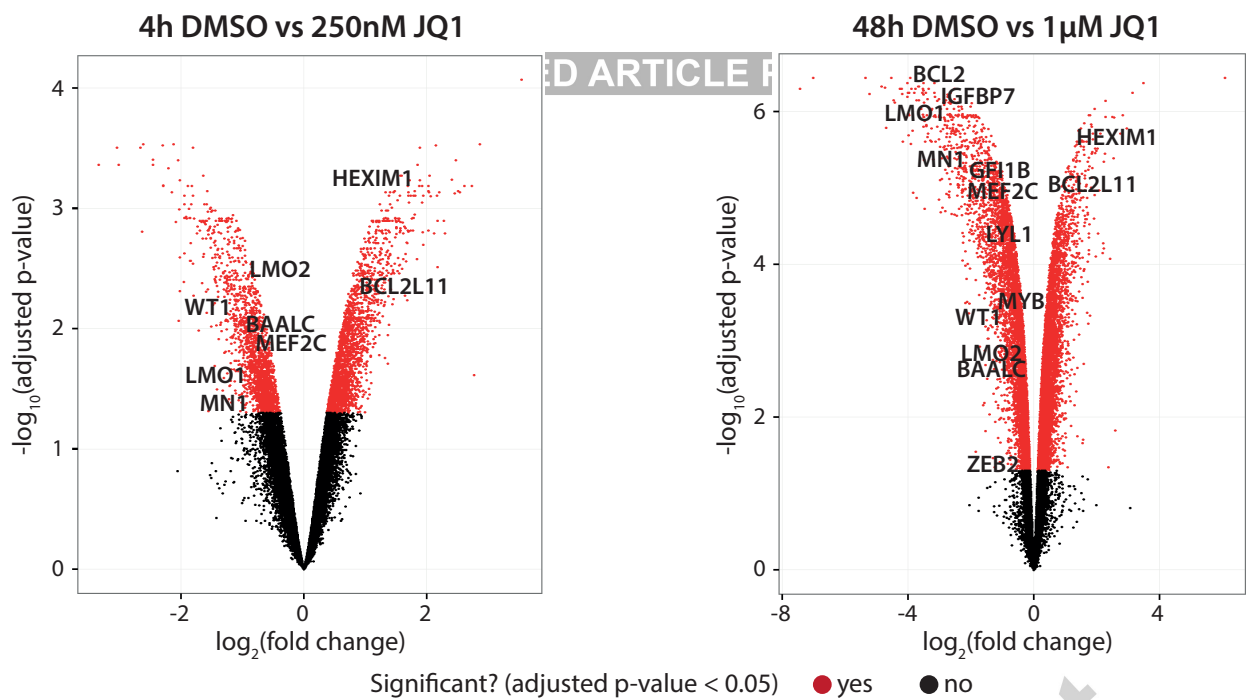
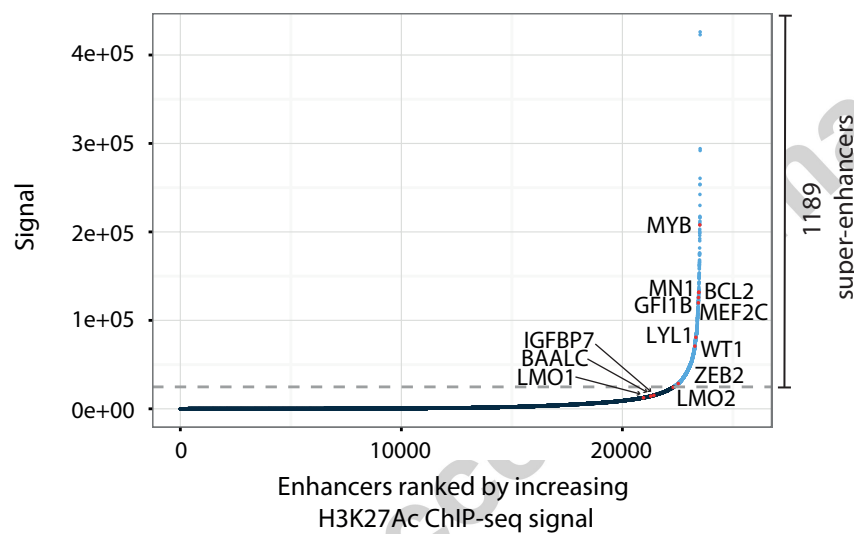


**Figure 5**

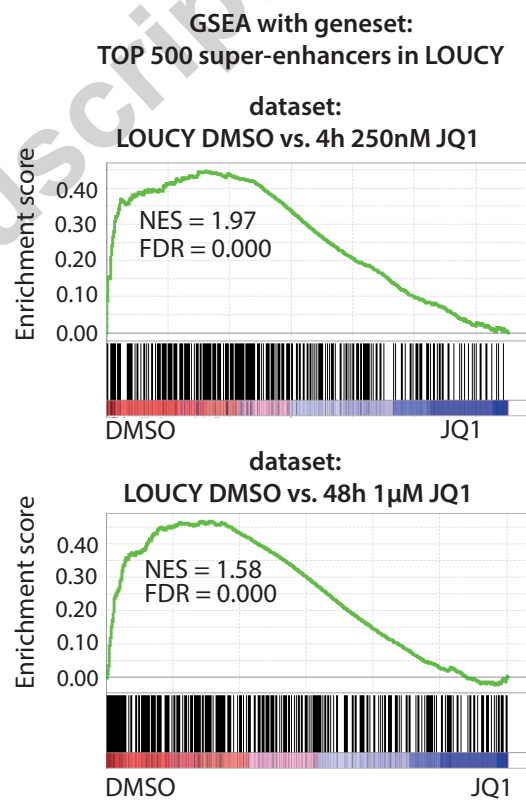
**A**



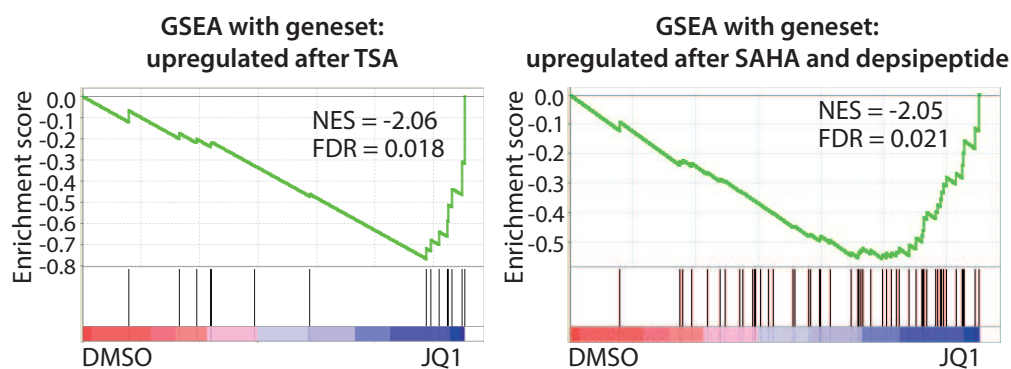
**B**

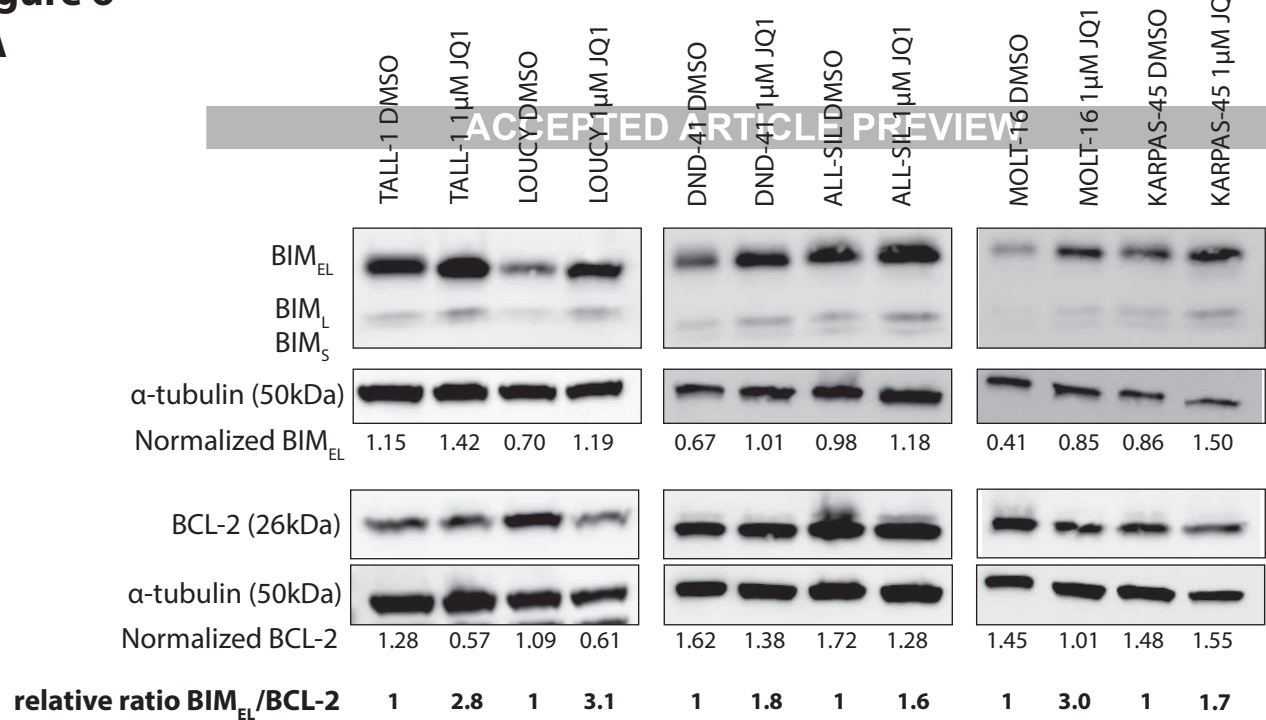
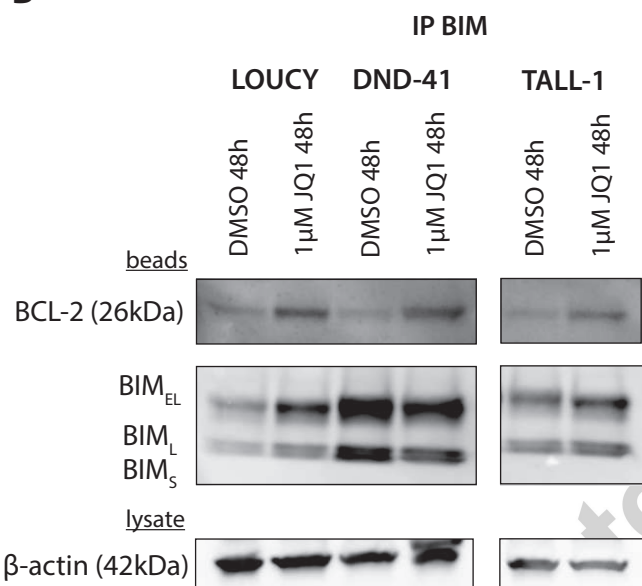
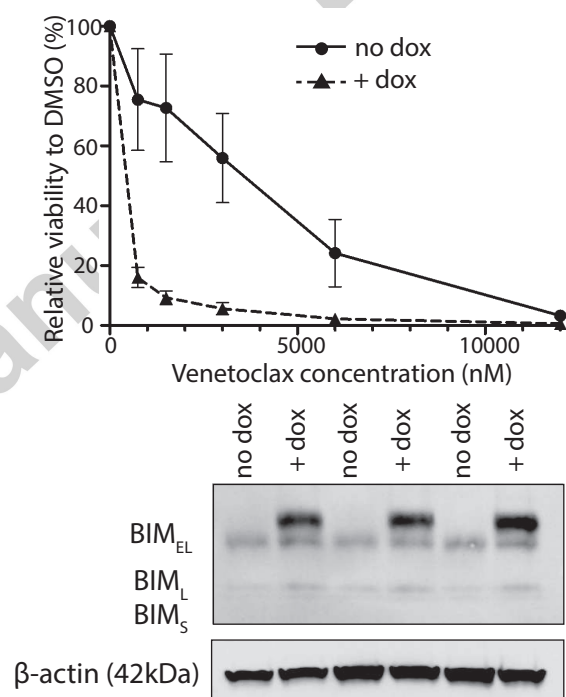


**C**



**D**



**Figure 6****A****B****C****D**